Supporting Information

Research on Advanced Photoresponsive Azobenzene Hydrogels with Push-Pull Electronic Effects: A Breakthrough in Photoswitchable Adhesive Technologies

Yun-Ying Wang, Peng-Wen Chen, Yu-Hsin Chen, Mei-Yu Yeh*

Department of Chemistry, Chung Yuan Christian University, No. 200, Zhongbei Rd., Zhongli Dist., Taoyuan City 320314, Taiwan, Republic of China.

*Corresponding author. E-mail: myyeh@cycu.edu.tw

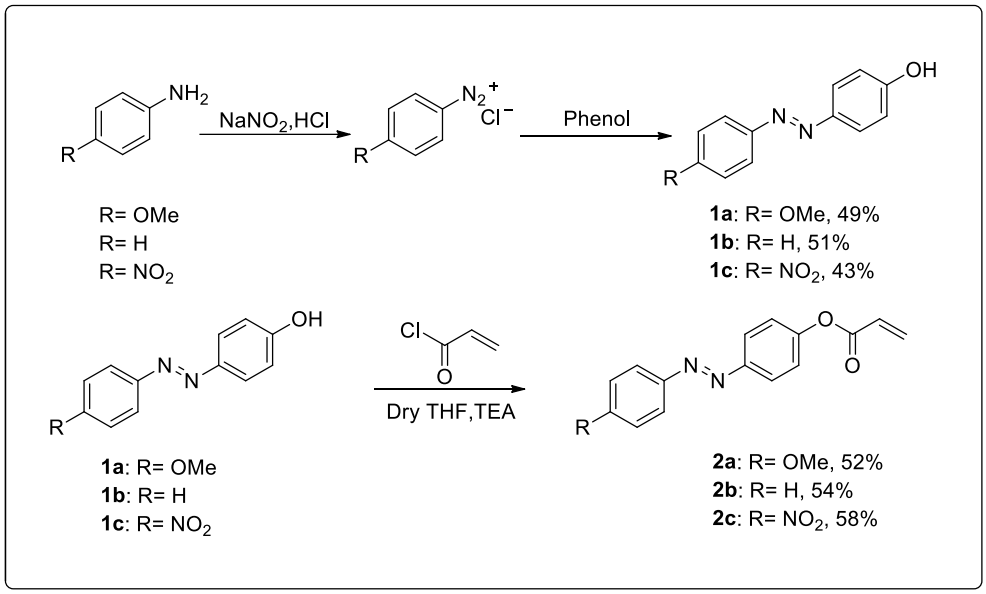

Scheme S1. Synthetic route for the monomers of ABOMe, ABH, and $ABNO_2$.

Synthesis of (*E*)-4-((4-methoxyphenyl)diazenyl)phenol (**1a**)

Dissolve *p*-anisidine (1.00 mL, 8.12 mmol) in a mixture of concentrated hydrochloric acid (2.00 mL, 64.66 mmol) and water (20 mL). Cool the solution to 5°C, then add dropwise an aqueous solution of sodium nitrite (0.80 g, 11.62 mmol) in 20 mL of water. Stir the reaction mixture at 5°C for 45 minutes, then add 2.5 mL of 1.0 M aqueous sodium hydroxide solution and phenol (1.112 g, 10.98 mmol). After stirring for 60 minutes, filter the precipitate, wash it with cold water, and dry it under vacuum to obtain an orange solid of **1a** (0.91 g, 49%). ^{1}H NMR (400 MHz, DMSO-d_6): δ= 7.81 (d, *J*= 9.2 Hz, 2H), 7.75 (d, *J*= 9.2 Hz, 2H), 7.10 (d, J= 9.2 Hz, 2H), 6.93 (d, J= 9.2 Hz, 2H).

Synthesis of (*E*)-4-(phenyldiazenyl)phenol (**1b**)

In a manner similar to that described above, a mixture of aniline (2.00 mL, 21.94 mmol), hydrochloric acid (2.00 mL, 64.66 mmol), sodium nitrite (1.60 g, 23.24 mmol) and phenol (2.22 g, 23.64 mmol) were converted to **1b** as an orange solid (2.19 g, 51%). ^{1}H NMR (400 MHz, $CDCl_3$): δ= 7.83-7.80 (m, 4H), 7.55-7.59 (m, 2H), 7.50-7.52 (m, 1H), 6.95 (d, *J*= 8.8 Hz, 2H)

Synthesis of (*E*)-4-((4-nitrophenyl)diazenyl)phenol (**1c**)

In a manner similar to that described above, a mixture of *p*-nitroaniline (2.00 g, 14.48 mmol), hydrochloric acid (2.00 mL, 64.66 mmol), sodium nitrite (1.60 g, 23.24 mmol) and phenol (2.22 g, 23.64 mmol) were converted to **1c** as an orange solid (1.48 g, 43%). ^{1}H NMR (400 MHz, DMSO-d_6): δ= 8.40 (d, *J*= 8.8 Hz, 2H), 8.00 (d, *J*= 8.8 Hz, 2H), 7.89 (d, *J*= 8.8 Hz, 2H), 6.99 (d, *J*= 8.8 Hz, 2H).

Synthesis of 4-methoxyazobenzene acrylate (ABOMe monomer, **2a**)

In a 100 mL two-neck round-bottom flask, dissolve compound **1a** (1.00 g, 4.39 mmol) in 12 mL of anhydrous tetrahydrofuran and 0.5 mL of triethylamine under a nitrogen atmosphere. After reacting for 30 minutes, acryloyl chloride (1.5 mL, 16.57 mmol) was added at 5°C, and the reaction mixture was continued for 24 hours. Add water and extract the mixture with dichloromethane, then collect the organic layer, concentrate it under reduced pressure, and dry it under vacuum. Purify the resulting material by column chromatography to obtain a yellow solid product of **2a** (0.59 g, 52%). ^{1}H NMR (400 MHz, DMSO-d_6): δ= 7.90-7.87 (m, 4H), 7.38 (d, *J*= 8.9 Hz, 2H), 7.12 (d, *J*= 8.9 Hz, 2H), 6.59-6.54 (m, 1H), 6.46-6.39 (m, 1H), 6.19-6.16 (m, 1H), 3.87 (s, 3H). ^{13}C NMR (100 MHz, DMSO-d_6): δ= 164.40, 162.56, 152.35, 150.21, 146.55, 134.43, 127.92, 125.10, 123.91, 123.18, 115.06, 56.09. HRMS (ESI$^+$) *m*/*z* for $C_{16}H_{14}N_2NaO_3$ [M+Na]$^+$, calcd 305.0902, found 305.0898.

Synthesis of azobenzene acrylate (ABH monomer, **2b**)

In a manner similar to that described above, a reaction mixture of **1b** (1.00 g, 5.05 mmol) and acryloyl chloride (1.5 mL, 16.57 mmol) were converted to **2b** as an orange solid (0.69 g, 54%). ^{1}H NMR (400 MHz, DMSO-d_6): δ= 7.96 (d, *J*= 8.8 Hz, 2H), 7.90-7.87 (m, 2H), 7.59 (d, *J*= 7.8 Hz, 3H), 7.42 (d, *J*= 8.8 Hz, 2H), 6.60-6.55 (m, 1H), 6.47-6.40 (m, 1H), 6.20-6.17 (m, 1H). ^{13}C NMR (100 MHz, DMSO-d_6): δ= 164.37, 152.93, 152.30, 150.10, 134.60, 132.12, 129.98, 127.90, 124.32, 123.37, 123.05. HRMS (ESI$^+$) *m*/*z* for $C_{15}H_{12}N_2NaO_2$ [M+Na]$^+$, calcd 275.0796, found 275.0795.

Synthesis of 4-nitroazobenzene acrylate ($ABNO_2$ monomer, **2c**)

In a manner similar to that described above, a reaction mixture of **1c** (1.00 g, 4.11 mmol) and acryloyl chloride (1.5 mL, 16.57 mmol) were converted to **2c** as a red solid (0.62 g, 58%). ^{1}H NMR (400 MHz, DMSO-d_6): δ= 8.42 (d, *J*= 8.7 Hz, 2H), 8.07-8.01 (m, 4H), 7.46 (d, *J*= 8.7 Hz, 2H), 6.60-6.56 (m, 1H), 6.47-6.40 (m, 1H), 6.20-6.18 (m, 1H). ^{13}C NMR (100 MHz, DMSO-d_6): δ= 164.28, 155.46, 153.87, 150.00, 148.96, 134.75, 127.80, 125.55, 124.99, 123.98, 123.55. HRMS (ESI^+) *m*/*z* for $C_{15}H_{12}N_3O_4$ $[M+H]^+$, calcd 296.0909, found 296.0908.

Biocompatibility of ABOMe, ABH, and $ABNO_2$ ionic hydrogels

The biocompatibility of ABOMe, ABH, and $ABNO_2$ ionic hydrogels was assessed by culturing L929 cells with an extraction medium.[S1] This medium was prepared by immersing the hydrogels in Dulbecco's Modified Eagle Medium (DMEM, Gibco, Life Technologies, Carlsbad, CA, USA) at a 1:10 volume ratio (hydrogel to medium) and incubating at 37 °C for two days. L929 cells were seeded in 96-well plates and cultured with DMEM at 37 °C under 5% CO_2 for one day. The DMEM was then replaced with the extraction medium, and the cells were allowed to grow for one, three, and five days. Cell viability assays were performed using the MTT reagent, and the optical density (OD) of the resulting solution was measured at 595 nm with a BioTek 800 TS microplate reader (Winooski, VT, USA). Cells not exposed to the test hydrogels served as the control group. The cell viability percentage (%) was calculated from the expression $OD_{sample}/OD_{control}$.

Porcine skin

Porcine skin tissues were purchased from a local market and stored at -20°C until needed. Before use, the fat was carefully trimmed off with a knife, and the cleaned skin was soaked in water and kept at 4°C.

Table S1. Formulations of azobenzene-based hydrogels.[a]

Hydrogel	AAM[b]	DF-PEG[b]	MAPTAC[b]	ABOMe[b]	ABH[b]	$ABNO_2$[b]
ABOMe hydrogel	45	2	/	1	/	/
ABH hydrogel	45	2	/	/	1	/
$ABNO_2$ hydrogel	45	2	/	/	/	1
ABOMe ionic hydrogel	45	2	2	1	/	/
ABH ionic hydrogel	45	2	2	/	1	/
$ABNO_2$ ionic hydrogel	45	2	2	/	/	1

[a]2,2'-azobisisobutyronitrile (AIBN, 0.4 %w/v), acrylamide is AAM, dialde-hyde-functionalized poly(ethylene glycol) is DF-PEG, and [3-(methacryloylamino)propyl]-trimethylammonium chloride is MAPTAC. [b]unit: %w/v

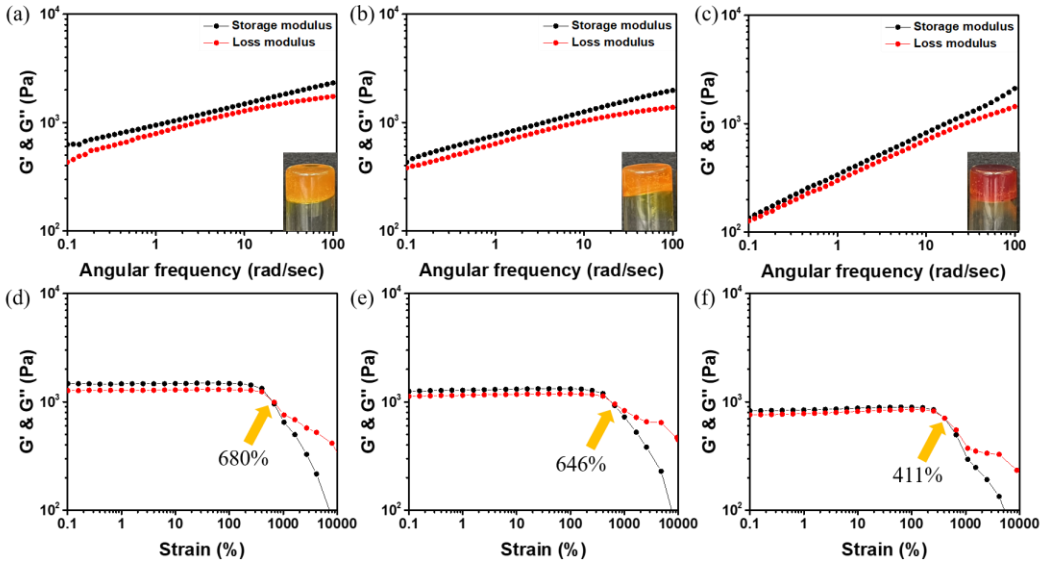

Fig. S1. Frequency dependent (ω = 0.1-100 rad/sec) of rheology measurement of (a) ABOMe hyderogel, (b) ABH hydrogel, and (c) $ABNO_2$ hydrogel. Inset: Optical images of the corresponding hydrogels. Strain dependent of G' (black) and G" (red) of (d) ABOMe hyderogel, (e) ABH hydrogel, and (f) $ABNO_2$ hydrogel.

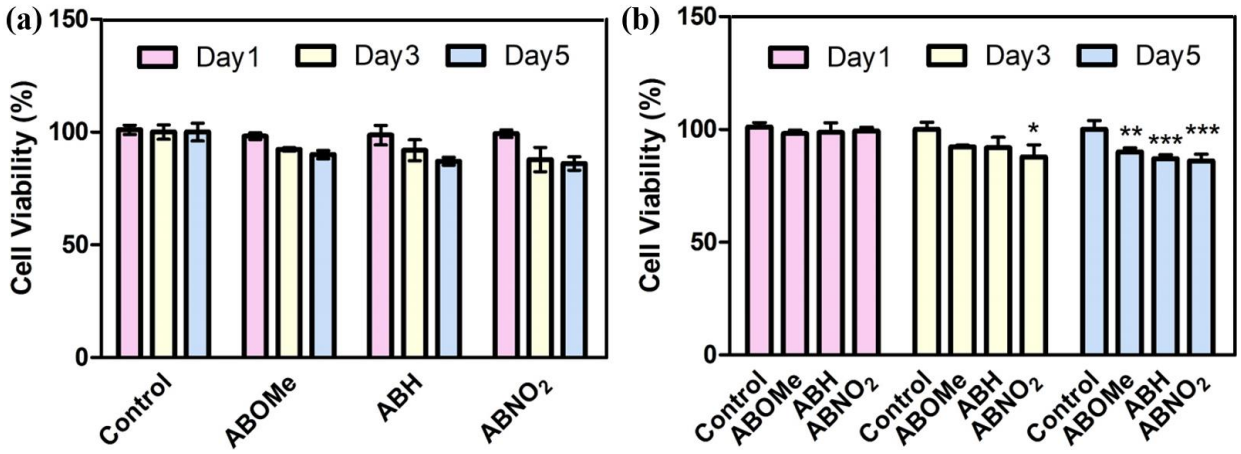

Fig. S2. Cell viability of L929 cells on ABOMe, ABH, and $ABNO_2$ ionic hydrogels for 1, 3, and 5 days. Statistical significance is indicated by *, **, or ***, representing $p < 0.05$, $p < 0.01$, and $p < 0.001$, respectively.

Note: The samples exhibited high cell viability, significantly exceeding the ISO standard for material cytotoxicity (70%).[S1,S2]

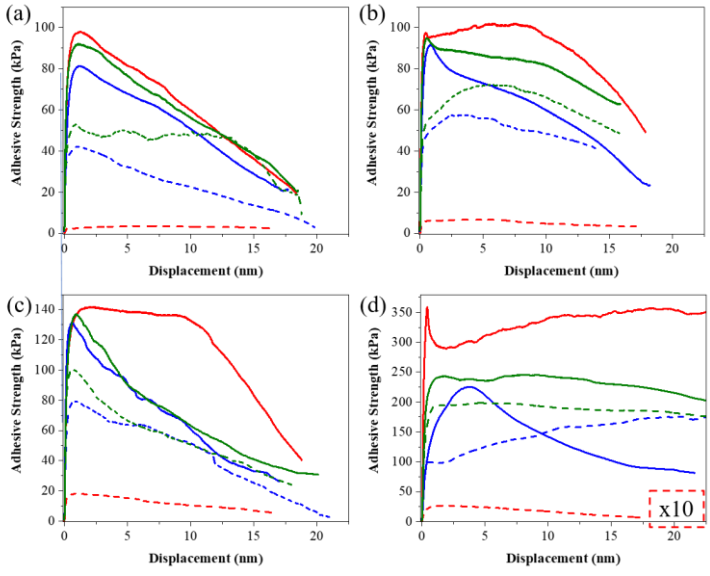

Fig. S3. Lap-shear strength tests for the adhesive strength of ABOMe (red), ABH (blue), and $ABNO_2$ (green) ionic hydrogels on (a) glass, (b) Al, (c) PVC, and (d) porcine skin before (solid line) and after (dashed line) UV light irradiation.

Table S2. Summary of lap-shear strength tests for the adhesive strength of ABOMe, ABH, and $ABNO_2$ ionic hydrogels on glass, Al, PVC, and porcine skin before and after UV light irradiation.

	ABOMe		**ABH**		**$ABNO_2$**	
Substrate	**before**	**after**	**before**	**after**	**before**	**after**
Glass	97.2 kPa	2.6 kPa	81.0 kPa	41.8 kPa	91.7 kPa	52.9 kPa
Aluminum	97.5 kPa	6.5 kPa	91.5 kPa	57.4 kPa	94.8 kPa	66.2 kPa
PVC	141.6 kPa	18.2 kPa	131.2 kPa	78.9 kPa	136.9 kPa	99.6 kPa
Porcine skin	360.7 kPa	2.5 kPa	222.6 kPa	100.1 kPa	241.6 kPa	193.9 kPa

Table S3 Comparison of reported adhesive strength values of hydrogels on porcine skin.

Component	**Maximum of adhesive strength (kPa)**	**Reference**
PDA-PAM/Mg^{2+} hydrogel	3.69 kPa	S3
0.05 NPs-P-PAA hydrogel	27.5 kPa	S4
BG/OSA hydrogel	55 kPa	S5
PDA-PAM hydrogel	15.2 kPa	S6
PAM-PEI hydrogel (PEI: PAM = 1: 9)	7 kPa	S7
PT-DA/PAA hydrogel	65 kPa	S8
HA-PEG hydrogel	30.3 kPa	S9
PAASP-40% hydrogel	120 kPa	S10
This work	360.7 kPa	/

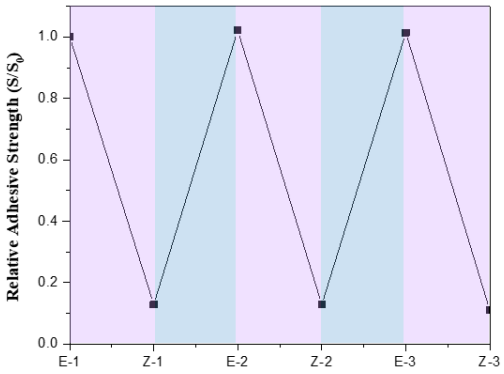

Fig. S4. Multicycle experiments monitoring the adhesive strength change of ABOMe ionic hydrogel under UV and visible light irradiation. S_0: original adhesive strength; S: adhesive strength after irradiation (purple background indicates UV light irradiation; blue background indicates visible light irradiation)

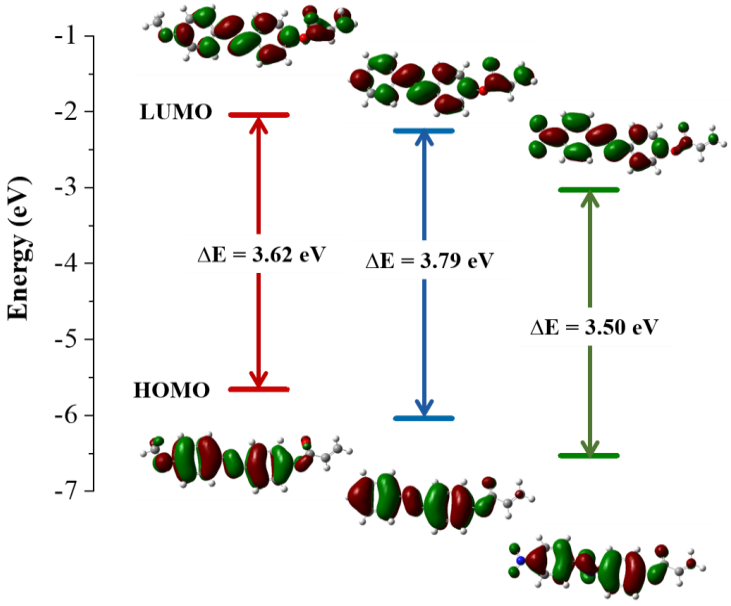

Fig. S5. Molecular orbital amplitude plots of HOMO and LUMO energy levels of (*E*)-ABOMe, (*E*)-ABH, and (*E*)-$ABNO_2$, calculated by using DFT at the B3LYP/6-31G(d) level.

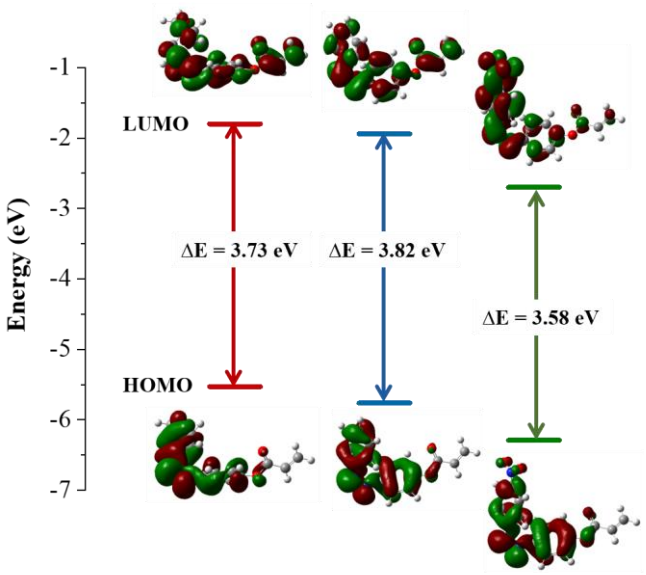

Fig. S6. Molecular orbital amplitude plots of HOMO and LUMO energy levels of (*Z*)-ABOMe, (*Z*)-ABH, and (*Z*)-ABNO$_2$, calculated by using DFT at the B3LYP/6-31G(d) level.

Table S4. Summarized the bond lengths (R), bond angles (A), and dihedral angles (D) of the *E* and *Z* isomers and the transition state (TS) of ABOMe, ABH, and $ABNO_2$, as determined using DFT at the B3LYP/6-31G(d) level.

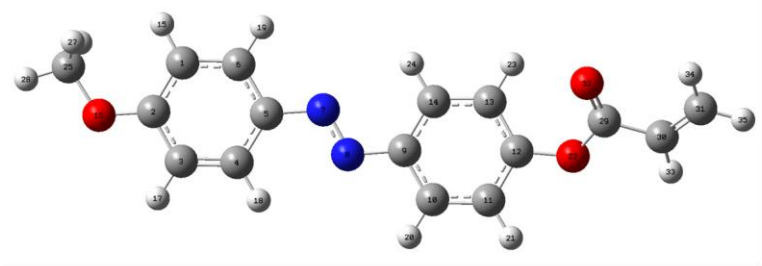

(*E*)-ABOMe

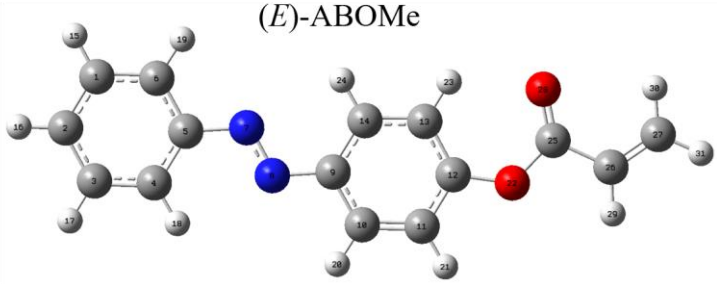

(*E*)-ABH

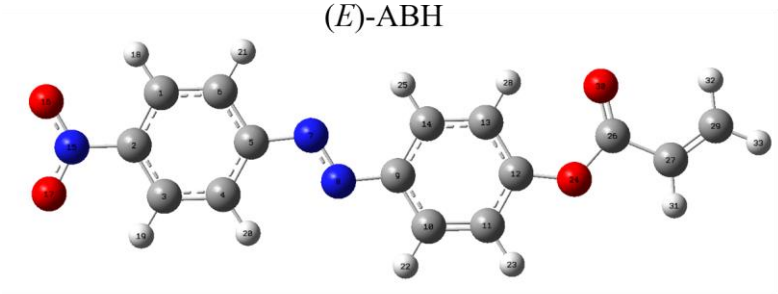

(*E*)-$ABNO_2$

	R (N7-N8)	A (C5-N7-N8)	D (C5-N7-N8-C9)
(*E*)-ABOMe	1.26360	115.05541	180.00002
(TS)-ABOMe	1.29210	123.99044	90.00806
(*Z*)-ABOMe	1.25108	124.76953	0.00538
(*E*)-ABH	1.26152	114.81494	179.93754
(TS)-ABH	1.22852	179.99985	89.06010
(*Z*)-ABH	1.24898	124.11442	0.06076
(*E*)-$ABNO_2$	1.26260	114.30772	178.96872
(TS)-$ABNO_2$	1.22596	179.90729	87.06676
(*Z*)-$ABNO_2$	1.24823	124.69824	0.00028

R: bond length in Å, A: bond angle in degrees, D: dihedral angle in degrees, E: energy in kcal/mol

Carbon, hydrogen, nitrogen, and oxygen atoms are depicted in gray, white, blue, and red, respectively.

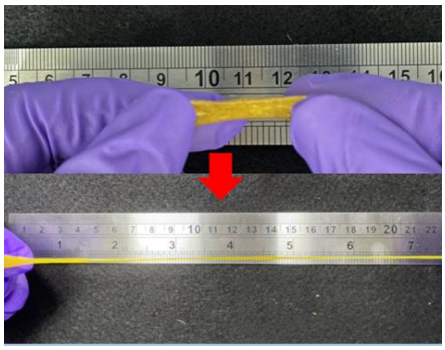

Fig. S7. The stretchability of the healed hydrogel.

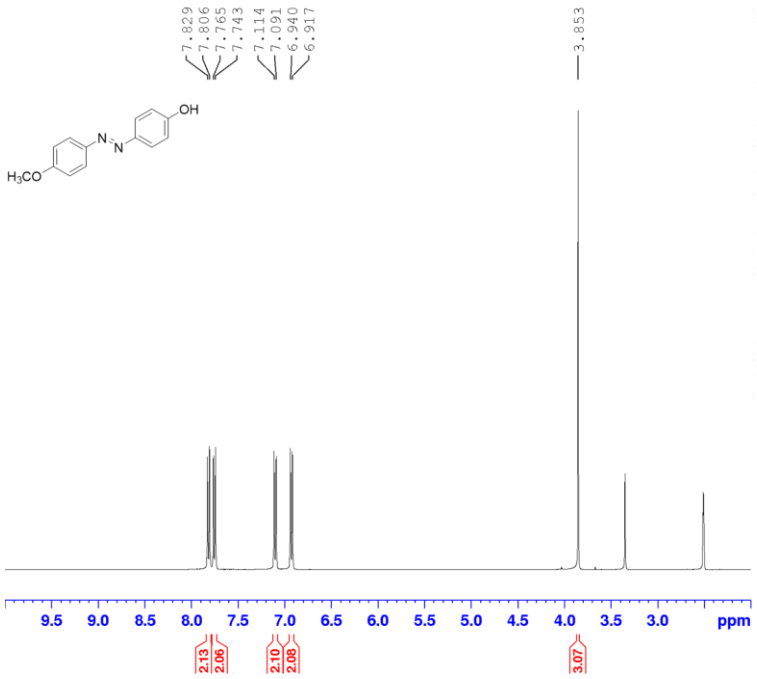

Fig. S8. ^{1}H NMR spectrum of compound **1a** in DMSO-d_6.

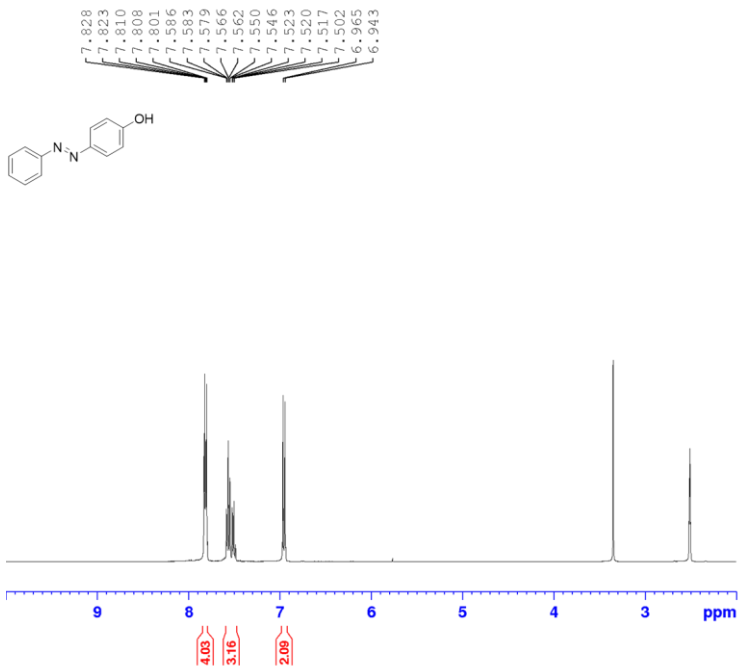

Fig. S9. ^{1}H NMR spectrum of compound **1b** in $CDCl_3$.

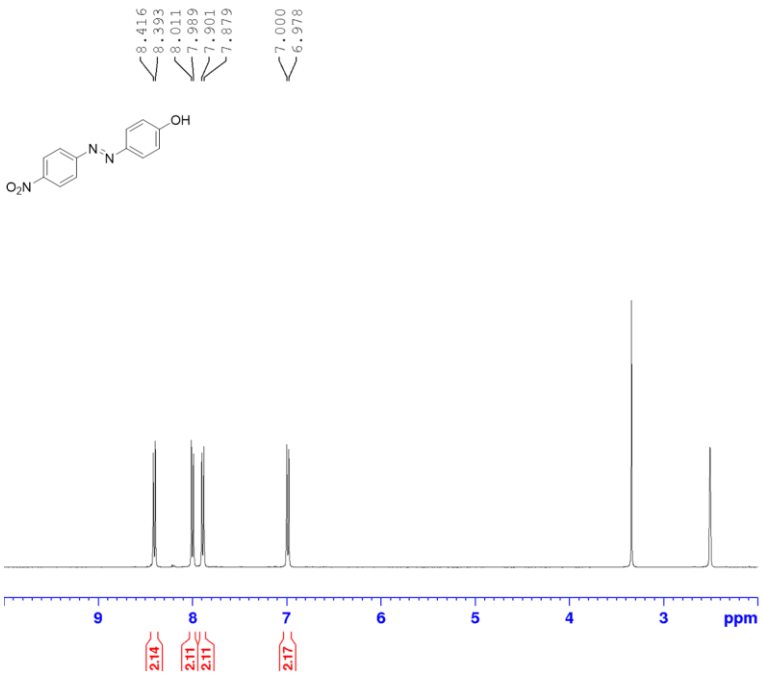

Fig. S10. ^{1}H NMR spectrum of compound **1c** in DMSO-d_6.

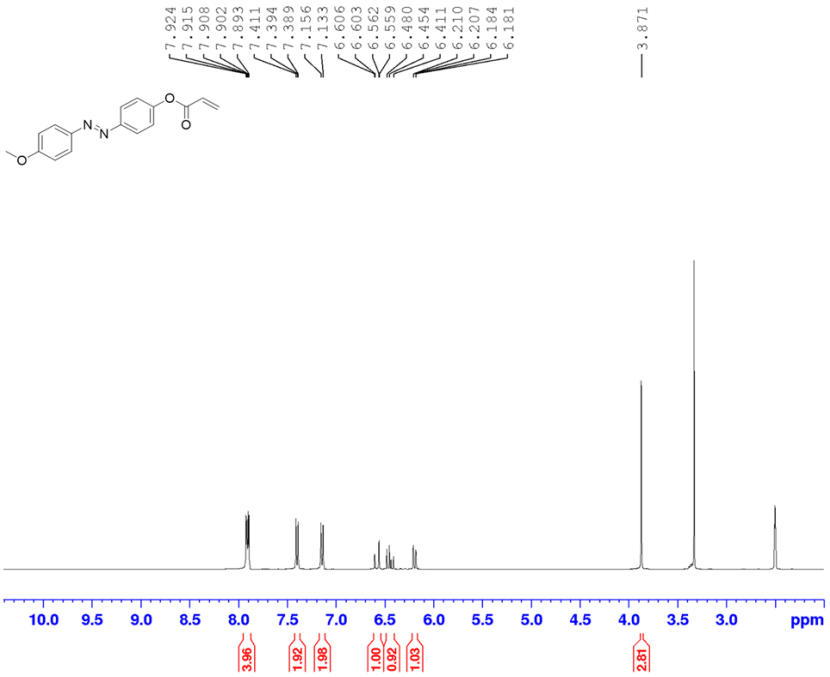

Fig. S11. ^{1}H NMR spectrum of ABOMe (**2a**) in DMSO-*d*$_6$.

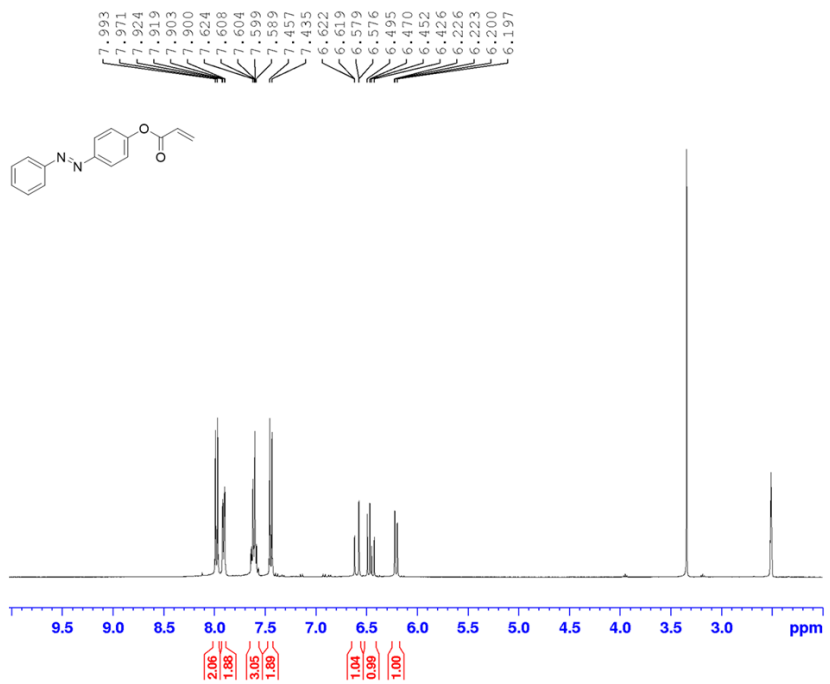

Fig. S12. ^{1}H NMR spectrum of ABH (**2b**) in DMSO-*d*$_6$.

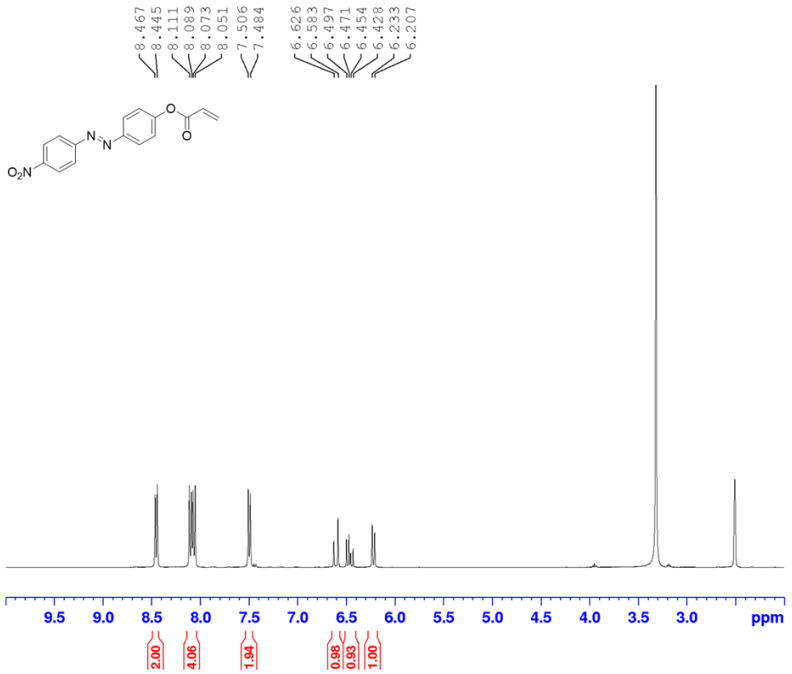

Fig. S13. ^{1}H NMR spectrum of ABNO$_2$ (**2c**) in DMSO-*d*$_6$.

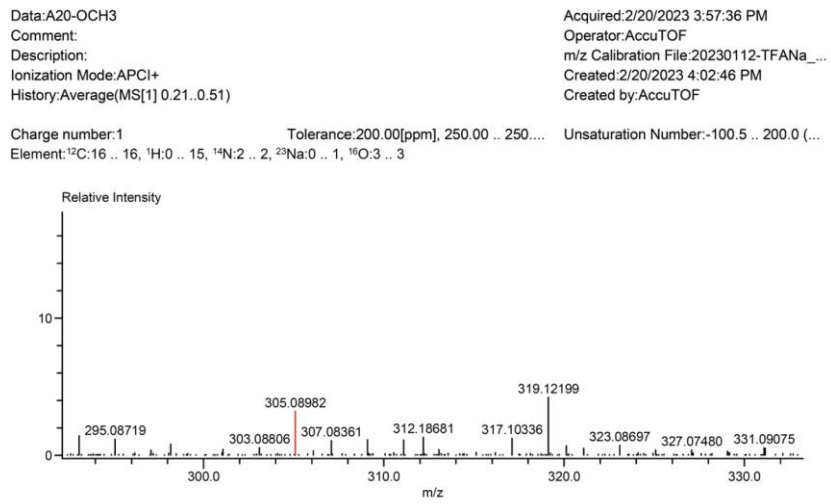

Mass	Intensity	Calc. Mass	Mass Difference [mDa]	Mass Difference [ppm]	Possible Formula
305.08982	1613.80	305.09021	-0.39	-1.29	$^{12}C_{16}{}^{1}H_{14}{}^{14}N_2{}^{23}Na_1{}^{16}O_3$

Fig. S14. HRMS spectrum of **2a**.

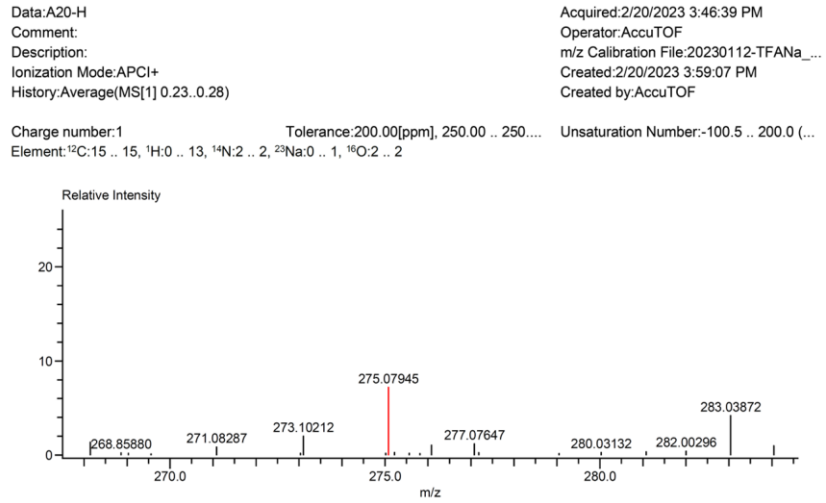

Mass	Intensity	Calc. Mass	Mass Difference [mDa]	Mass Difference [ppm]	Possible Formula
275.07945	5699.90	275.07965	-0.20	-0.71	$^{12}C_{15}{}^{1}H_{12}{}^{14}N_{2}{}^{23}Na_{1}{}^{16}O_{2}$

Fig. S15. HRMS spectrum of **2b**.

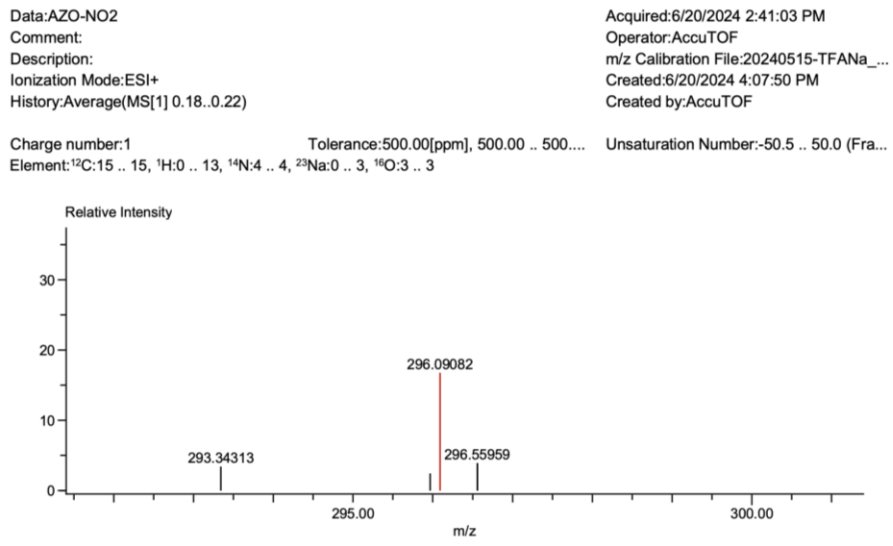

Mass	Intensity	Calc. Mass	Mass Difference [mDa]	Mass Difference [ppm]	Possible Formula
296.09082	614.73	296.09094	-0.12	-0.40	$^{12}C_{15}{}^{1}H_{12}{}^{14}N_{4}{}^{16}O_{3}$

Fig. S16. HRMS spectrum of **2c**.

Reference

S1. ISO 10993-5: 2009 Biological Evaluation of Medical Devices-Part 5: Tests for in Vitro Cytotoxicity (International Organization for Standardization, 2009).

S2. S. Prasadh, M. Gupta and R. Wong, *Sci. Rep.*, 2022, **12**, 8259.

S3. Z. Guo, Z. Zhang, N. Zhang, W. Gao, J. Li, Y. Pu, B. He and J. Xie, *Bioact. Mater.*, 2022, **15**, 203-213.

S4. D. Gan, W. Xing, L. Jiang, J. Fang, C. Zhao, F. Ren, L. Fang, K. Wang and X. Lu, *Nat. Commun.*, 2019, **10**, 1487.

S5. L. Gao, Y. Zhou, J. Peng, C. Xu, Q. Xu, M. Xing and J. Chang, *NPG Asia Mater.*, 2019, **11**, 66.

S6. L. Han, L. Yan, K. Wang, L. Fang, H. Zhang, Y. Tang, Y. Ding, L.-T. Weng, J. Xu, J. Weng, Y. Liu, F. Ren and X. Lu, *NPG Asia Mater.*, 2017, **9**, e372.

S7. Y. Yan, S. Xu, H. Liu, X. Cui, J. Shao, P. Yao, J. Huang, X. Qiu and C. Huang, *Colloids Surf. A*, 2020, **593**, 1246.

S8. S. Kindaveeti, G. Choi, S. C. Veerla, S. Kim, H. J. Lee, U. Kuzhiumparambil, P. J. Ralph, J. Yeo and H. E. Jeong, *Nano Converg.*, 2024, **11**, 12.

S9. H. Ren, Z. Zhang, X. Cheng, Z. Zou, X. Chen and C. He, *Sci. Adv.*, 2023, **9**, 4327.

S10. J. Yu, Y. Qin, Y. Yang, X. Zhao, Z. Zhang, Q. Zhang, Y. Su, Y. Zhang and Y. Cheng, *Bioact. Mater.*, 2023, **19**, 703-716.